06

Microwave synthesis method for obtaining temperature-activated carbon materials

© I.G. Dyachkova,[1] D.A. Zolotov,[1] A.S. Kumskov,[1] I.S. Volchkov,[1] E.V. Matveev,[2] V.E. Asadchikov[1]

[1] National Research Center „Kurchatov Institute“, Moscow, Russia
[2] Research Institute of Advanced Materials and Technologies,
105187 Moscow, Russia
e-mail: sig74@mail.ru

Received October 19, 2023
Revised April 15, 2024
Accepted April 16, 2024

In this work, the microwave synthesis of activated carbon material from cotton lint samples was developed and improved, with the priority task of determining the conditions and performance of „full activation“ during microwave carbonization. Using such methods as optical and electron microscopy, X-ray microtomography, X-ray fluorescence analysis, X-ray phase analysis and evaluation on methylene blue adsorption, morphology, elemental and phase compositions, as well as adsorption capacity of carbonized cotton lint samples at different microwave exposure modes were investigated. It is experimentally shown that microwave activation can be carried out in a single step. It is assumed that a deeper degree of purification or the use of purer raw materials will allow to achieve higher adsorption capacity values.

Keywords: cotton lint, microwave, carbonization, activation.

DOI: 10.61011/TP.2024.06.58823.266-23

Introduction

One of heating methods used in production of porous carbon materials is microwave (MW) exposure [1,2]. Various processes occurring under microwave exposure, such as pyrolysis, carbonization, activation, are determinant for the quality of the produced activated carbon materials (ACM) [2–5]. The recent developments in the class of porous carbons — ACM, made of biomass, which are traditionally used as adsorbents or catalysts, have currently found wide application in production of materials for hydrogen accumulation and supercapacitors [6,7]. These activated carbons have an improved shape (resistance of macro/meso/microporous carbon) and better properties (chemical and thermal stability, low density). Besides, the above carbon materials differ by environmental friendliness, availability, and simplicity and cost-effectiveness of their treatment [7,8].

In connection with the growing demand for activated carbons in traditional fields of application and development of new technologies using these materials, in the context of the relevant energy and environment situation, reduction of energy costs and environmental impact of the processes used for production and regeneration of ACM, is of principal importance [9]. The process of activated carbons production consists of the raw materials carbonization and activation stages.

Main methods of carbonization and activation of carbon materials may be divided into chemical (impregnation with acids and alkali), physical or thermal (activation at high temperature in the environment of air, water vapor or CO_2) and physicochemical (combination of both methods, for example, carbonization by heating of the raw materials impregnated with a reagent with subsequent physical activation in an oxygen-containing medium).

Chemical activation is usually preferable because of simplicity, higher speed of activation, higher yield, lower process temperature and better development of the porous structure. Besides, the disadvantages of the chemical activation include corrosion activity of reagents and the need to flush the product.

Traditional thermal furnaces or microwave (MW) heating units may be used as heat sources in all the specified methods. Recently the microwave method of heating in combination with the chemical impregnation of the raw materials becomes the alternative to the traditional method of treatment owing to faster, selective, even and volume heating, and higher controllability. MW heating increases carbon yield, improves quality of activated carbons, provides for high energy efficiency, minimizes formation and emission of hazardous substances, thus making the technology more environmentally friendly. Therefore, this technology seems to be an energy efficient alternative solution for production of finished materials [10–12]. Besides, use of microwave heating in ACM production makes it possible to obtain some advantages, namely reduction of time to process the raw materials (precursors) [13–15], volume nature of heating [16], increased porosity of the surface of activated carbons [17], absence of the need to grind the source raw materials [5] etc.

However, in virtue of disordered nature and local heterogeneity, description of the activated carbon microstructure is complicated. Defective plates of graphene type are seen as elementary building blocks of these carbon materials.

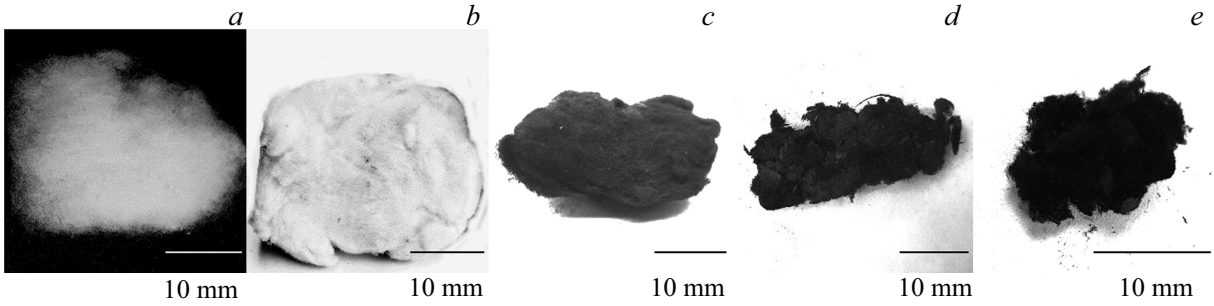

Figure 1. Photographs of studied specimens of cotton linter: *a* — source (№ 1); *b* — treated with 5% solution ofH_3PO_4 (№ 2); *c* — MW-carbonized (№ 3); *d* — MW-carbonized with partial activation (№ 4); *e* — MW-carbonized with partial activation (№ 5).

Individual graphene-like layers are often folded together at a very short length, which causes formation of domains, where layer-to-layer spaces form microporosity (micropores with size from 0.4 to 2 nm). Cavities between randomly arranged domains cross-linked together form, depending on their size, supermicroporosity and mesopores (from 2 to 100−200 nm) ACM [18–20]. Mesopores arise as a result of organization of nanosize domains or even individual parties comprising several domains, and also as a result of impact of natural (mineral fraction) and added (activated agents) inclusions [21,22]. Thus, as of today the optimization of ACM characteristics of nearly almost of empirical nature.

Nevertheless, based on multiple experimental data, one may select methods and modes for synthesis of ACM with characteristics required for specific application. This paper is aimed at development and improvement of MW synthesis of ACM from precursors of plant biomass for use in energy storage systems with the priority objective to define the conditions and perform „full activation" during MW carbonization. The physical sense of „full activation" consists in most complete removal of resins and other high-molecular products of pyrolysis from the pores of carbon material, which increases the area of its active surface. For this purpose this paper studied morphology, elementary and phase composition, and also adsorption capacity of specimens of carbonized cotton linter at various modes of MW exposure. A complex approach was applied using such methods as optical and electron microscopy, X-ray micro-tomography, X-ray fluorescence analysis, X-ray diffraction analysis and evaluation of adsorption using methylene blue.

1. Specimens and research methods

Carbon-based material was cotton linter being textile industry waste. Source specimens were test portions of while cotton linter with dry mass of 3.0 g (Fig. 1, *a*, specimen № 1). The activating agent for additional chemical activation was orthophosphoric acid H_3PO_4 (pure orthophosphoric acid GOST 6552-80; manufactured by Chongqing Chuandong Chemical (Group) Co., Ltd, China). This activator provides minimum impact on the environment [23]. Besides, orthophosphoric acid depolymerizes cellulose, hemicellulose and lignin, stimulates formation of cross links between carbon polymers via reactions of dehydration and condensation, stimulates formation of phosphates and polyphosphates, binding biopolymer fragments, helps to expand micro- and mesopores in the activated carbon [24,25]. Specimens were impregnated with 5% solution of H_3PO_4 over a pan of simmering water at 97°C, 1.5 h, squeezed and shaped as balls with diameter of ∼ 30 mm, weight of ∼ 9 g in moist condition (Fig. 1, *b*, specimen № 2). This concentration value (5% H_3PO_4) was determined empirically using the temperature dynamics of the process of MW treatment (temperature was determined using the method of spectral pyrometry), percentage of yield of carbon material after carbonization and integral adsorption capacity of activated carbon materials. It was found that in general the lower concentration H_3PO_4 decreases the percentage of product yield due to high degree of combustion loss, and higher concentration adversely impacts the temperature dynamics of MW carbonization — the process of MW carbonization and activation is less stable.

The process of microwave pyrolysis carbonization was carried out both in the inert gas medium, for which argon gas was used, and without one. Besides, the composition of the working gas medium was selected empirically, based on the preliminary multiple experiments, aiming for its stability and discharges under the conditions of exposure to MW electromagnetic field.

Upon completion of carbonization, all specimens were photographed and weighed. The weighing procedure was carried out on a laboratory scale BM313M-II OKB Vesta with precision of 1 mg and maximum measured weight of 310 g.

MW treatment of the cotton linter specimens was carried out in a resonating MW chamber of beam type and MW plant of waveguide type (FSBSI RIAMT). During the tests in the resonating MW chamber the specimen impregnated in 5% H_3PO_4, was carbonized in the media of argon Ar, 10 min, and carbon dioxide CO_2, 10 min (Fig. 1, *c*, specimen № 3). In case of full carbonization, the cotton linter specimen becomes graphite grey. Mass of the specimen № 3 after carbonization was 0.785 g. The process of MW carbonization with partial activation of the specimen impregnated in 5% H_3PO_4, was carried out in medium of

CO_2 5 min and 2 min on air (Fig. 1, *d*, specimen № 4). The residual mass of this specimen was 0.308 g. Visually areas of two colors may be identified in the volume of this specimen — deep black and graphite-grey. It is assumed that large depth of „black color" in partially activated areas is caused by the fact that the surface of cotton fibers becomes more developed (the number of micro-, meso- and macropores increases), and the visible light is absorbed by it to a large extent vs the areas that do not have such a developed surface (they look more grey). Therefore, during MW carbonization due to higher process reaction rates a structure of heterogeneous volume is formed.

Completion of „full" activation characterized by higher homogeneity of properties (adsorption, porosity, elemental composition) in the entire volume of the specimen requires achievement of higher uniformity and creation of maximum possible density of electromagnet field capacity flow in the spatial area of microwaves and specimen interaction. Preliminary calculations and analysis of literature [26] confirmed that it was therefore more efficient to use a waveguide MW system, for which purpose a new plant was designed on the base of FSBSI RIAMT using a single-mode rectangular waveguide operating at frequency $f = 2.45$ GHz. The size of the specimen for this unit was limited by dimensions of the operating area (18×45 mm). Therefore, a cotton linter specimen was taken for the tests with weight of 1.0 g, which after impregnation with 5% solution of H_3PO_4 was squeezed and shaped in the form of a cylinder with diameter of ~ 15 mm, height of 40 mm and weight of ~ 2.9 g in moist condition. Further the specimen placed in a quartz tube was carbonized in an MW unit in medium of CO_2 for 180 s (Fig. 1, *e*, specimen № 5). The weight of carbonized specimen was 0.110 g.

To determine adsorption capacity of MW carbonized samples, a spectrophotometric method was used, by intensity of light absorption. The research was carried out using methylene blue (MB) indicator according to GOST 4453-74N [27]. Light absorption intensity is characterized by optical density. If the thickness of the dyed substance layer is invariable, and at certain length of light wave (665 nm, so that absorption is maximum), the optical density is directly proportionate to substance concentration. Optical density of the analyzed sample was measured, and, using a calibration chart (chart of optical density dependence on the solution concentration), substance concentration in the sample was defined. Adsorption capacity of MB — characteristic of adsorbent showing the maximum mass of adsorbate (methylene blue dye) that the adsorbent may adsorb on the surface, [mg/g]. Besides, the carbon material is deemed to be activated, if its adsorption capacity exceeds 225 mg/g (GOST 4453-74). In this paper local or integral values of specimens' adsorption capacity were determined for different conditions of carbonization. For local estimate, the sample of the required volume of the specimen (№ 4,5) was taken from the areas of most intense black color. For integral estimate of adsorption capacity the sample (№ 3) was ground manually with a blade to fragments with size of < 0.15 mm (assessment of dimensions by SEM images), which made it possible to avoid „sticking" of powder when dosed and to provide the optimal area of available surface. The produced powder was mixed, and the necessary volume was sampled.

Specimens of carbon materials were studied in optical microscope (OM) Biolam M-1 (LOMO, Russia) in reflected light. Images were recorded using camera TS-1000 with maximum resolution 3664×2748 and sensitive element 10 Mp, 1/2" CMOS. Increase of plan achromatic correction lens was 10-, 40- and 100 -fold, and maximum resolution — around 0.05 μm.

X-ray tomographic (XRT) studies were carried out using microtomograph „TOMAS" (Federal Scientific and Research Center „Crystallography and Photonics" Russian Academy of Sciences, Russia) [28]. Experiment parameters: tube Cu (focus size 20×2.0 mm, mode 40 kV×40 mA); wavelength — 1.54 Å(E = 8.047 keV); monochromator — pyrolytic graphite, reflection (0001); detector Ximea Xi-Ray11 (pixel size $9 \times 9\,\mu$m, field of vision 36×24 mm); exposure — 3.5 s per projection; measurement range — 400 projections with pitch 0.5° (0°−200°).

Studies of the elemental composition of specimens were carried out using X-ray microtomograph „DITOM-M" (Federal Scientific and Research Center „Crystallography and Photonics" Russian Academy of Sciences, Russia) [29] by method of X-ray fluorescence analysis (XRFA). Experiment parameters: tube Cu (focus size 20×2.0 mm), mode 40 kV×40 mA; wavelength — 1.54 Å(E = 8.047 keV); monochromator — silicon, reflection (111); beam size — 8.0×1.0 mm; detector-spectrometer Amptek 123SDD (lower limit ~ 1 keV, energy resolution ~ 150 eV); exposure — 600 s per measurement.

The methods of scanning electron microscopy (SEM) and transmission electron microscopy (TEM) with the possibility of energy-dispersive X-ray microanalysis (EXM) were used to study the structure and chemical composition of individual fibers and fibrils of carbonized specimens of cotton linter. Autoemission scanning electron microscope FEI Scios (Thermo Fisher Scientific, USA, Everhart–Thornley) was used in the modes of secondary electrons, at accelerating voltages from 2 to 20 kV, as well as transmission electron microscope with field emission FEI Tecnai Osiris (Termo Fisher Scientific, USA) at accelerating voltage of 200 kV. The transmission electron microscope is equipped with a system of detectors making it possible to obtain the maps of distribution of chemical elements in the large area for several minutes. Specimens for TEM studies were dispersed in acetone by ultrasound and applied on copper lattices with micro-performed amorphous carbon films (SPI, USA).

Studies of the specimens phase composition were carried out on X-ray diffractometer MiniFlex 600 (Rigaku, Japan). Experiment parameters: tube Cu, mode 40 kV×15 mA; wavelength — 1.54 Å ($E = 8.047$ keV); scanning $\theta-2\theta$-mode; interval of angles $2\theta = 10-40°$, pitch 0.01°; exposure — 1 s per increment.

Phases were identified using databases ICDD PDF-4 [30].

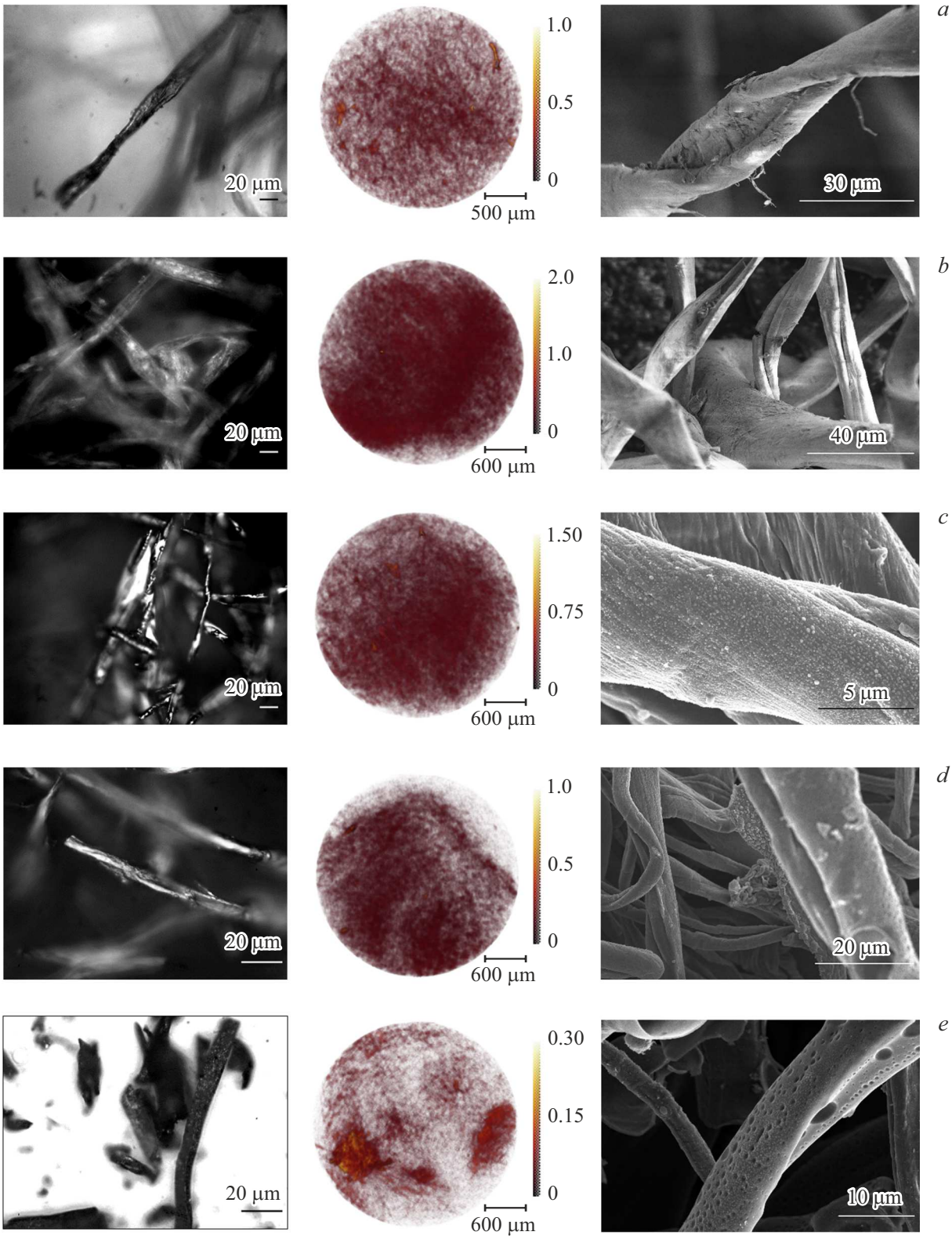

Figure 2. Optical (on the left), XRT (in the center) and SEM (on the right) images of cotton linter specimens: *a* — source (№ 1); *b* — treated with 5% solution ofH_3PO_4 (№ 2); *c* — MW-carbonized (№ 3); *d* — MW-carbonized with partial activation (№ 4); *e* — MW-carbonized with partial activation (№ 5).

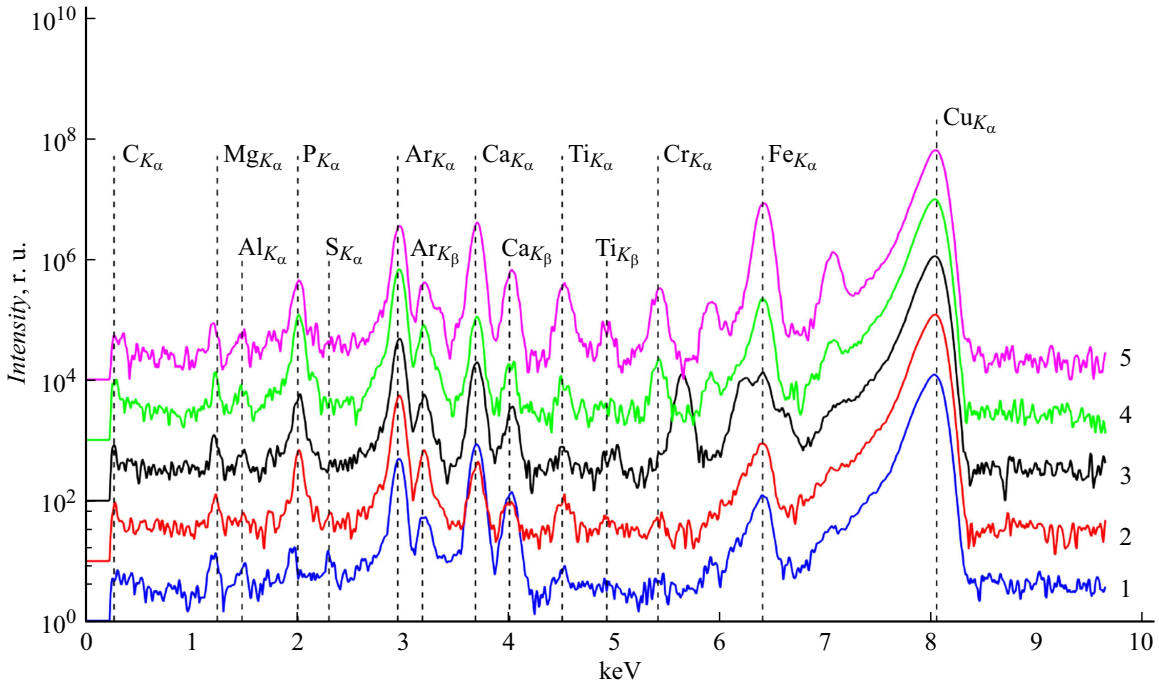

Figure 3. X-ray fluorescence spectra of studied cotton linter specimens: № 1 — source; № 2 — treated with 5% solution H_3PO_4; № 3 — MW-carbonized; № 4 — MW-carbonized with partial activation; № 5 — MW-carbonized with partial activation. Peaks from Ar (air) and Cu (X-ray tube anode) are instrumental. Spectra are separated ($\times 10$) along axis of intensity for visualization.

2. Results and discussion

Measurements of integral adsorption of fully MW carbonized specimen (№ 3, graphite grey color) yielded the value of its adsorption capacity by methylene blue 126 mg/g. In process of specimen (№ 4) heating in a chamber MW unit of beam type using a two-stage processing mode of CO_2+air, its complete carbonization took place (the specimen becomes graphite grey), and certain areas demonstrate deeper „black“ color. As local adsorption measurements have shown, these areas have higher adsorption capacity by MB 451 mg/g. This made it possible to conclude on the correlation of „black“ color depth and adsorption capacity, which may indicate partial activation in these areas. Specimen № 5, for which an attempt was made to implement „full activation“ in one stage in medium CO_2 using a waveguide MW unit, is also heterogeneous in volume and contains areas that underwent carbonization (graphite grey color) and activation (black color). Measured local adsorption capacity of areas with „black“ color in specimen № 5 turned out to be comparable to the value obtained for specimen № 4, and made 452 mg/g.

The results of the study of cotton linter specimens fiber structure and morphology variation in process of pyrolysis MW carbonization are shown in Fig. 2.

Analysis of the data obtained by various methods makes it possible to make the following conclusions. Fibrillar structure is well seen on the surface of cotton linter specimens' fibers. Fibrils are located in parallel to each other and are twisted in a screw-like manner at the angle relative to the fiber axis. Fiber width is from 3 to 20 μm. Fibers of specimen № 4 have pores with size from hundreds of nanometers to units of micrometers (Fig. 2, *d*). For specimen № 5 a well-developed, porous surface of the fiber is observed (Fig. 2, *e*) with pore size from several dozens to several hundreds of nanometers. Which is confirmed by minimum absorption ratio $\mu \sim 0.3\,\mathrm{mm}^{-1}$ (XRT image) compared to other studied specimens. Besides, the fiber maintains the shape integrity.

From the images shown in Fig. 2 one may conclude that all studied specimens are contaminated. Besides, the presence of mineral substances and microelements in cotton linter is natural. The XRT image of the source specimen (Fig. 2, *a*) contains areas with increased absorption ratio $\mu \sim 1.5\,\mathrm{mm}^{-1}$ vs the main volume. However, after MW carbonization as well there are contaminations observed in the form of impurities, which are deposited on fibers of the outer surface of the specimen and fibers of near-surface layer (Fig. 2, *c*–*e*). Probably, the rapid MW heating causes simultaneous high concentration of liquid and volatile products of pyrolysis, which migrate and are partially deposited on the fiber surface. This, in its turn, results in fiber closure with formation of solid structures that complicate further release of pyrolysis products from the specimen volume.

Impurities that may be present in the studied specimens of cotton linter may be divided into three groups by origin: elements of mineral nutrition; contamination of cotton fibers in process of growth and storage; chemical reagents used to prepare specimens for carbonization process. As you can see from XRFA spectra in the source specimen (Fig. 3, № 1) the following macro- and microelements are

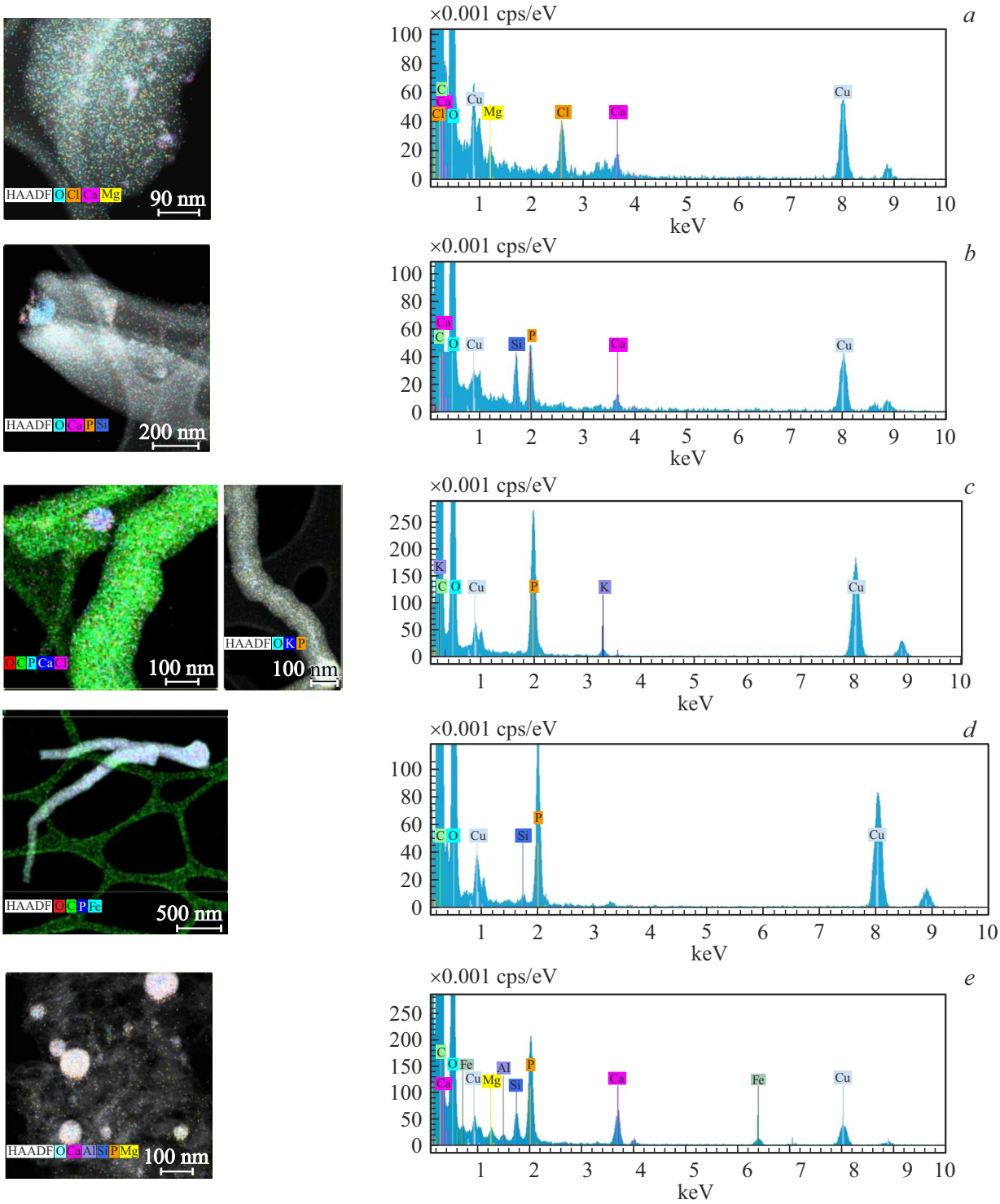

Figure 4. Maps of element distribution and SEM spectra for specimens of cotton linter: *a* — source (№ 1); *b* — treated with 5% solution ofH_3PO_4 (№ 2); *c* — MW-carbonized (№ 3); *d* — MW-carbonized with partial activation (№ 4); *e* — MW-carbonized with partial activation (№ 5).

present, which are related to mineral nutrition of plants: Mg, Al, P, S, Ca, Fe. According to EXM data (Fig. 4, *a*) the elemental composition of typical contaminants (O, Cl, Ca, Mg) in different combinations and proportions complies with the list of micro- and macroelements of cell nutrition, which indicates their mostly natural origin. Copper peaks on EXM spectra comply with the lattice for SEM studies. After the preliminary treatment of cotton linter specimens in 5%-th aqueous solution of orthophosphoric acid, some contaminants are removed from

Quantitative analysis of elemental composition of specimen № 5

Element	Weight %	Atom %
C	93.00	95.54
O	4.73	3.65
Al	0.08	0.04
Si	0.12	0.05
P	0.99	0.40
K	0.07	0.02
Ca	0.94	0.29
Fe	0.07	0.01

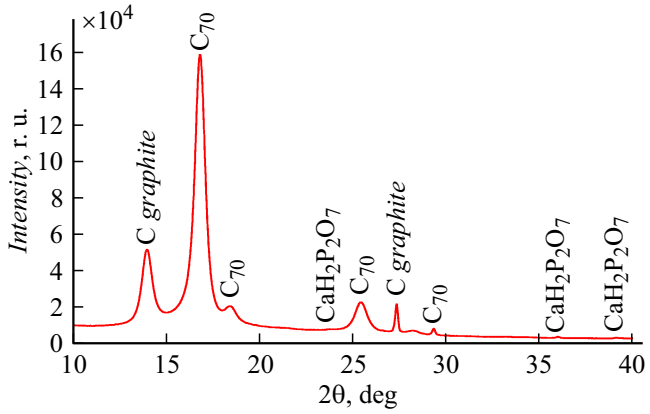

Figure 5. X-ray pattern of specimen № 5.

the specimen, and phosphorus content increases at the same time (Fig. 3,№ 2), which is confirmed by SEM spectra (Fig. 4, *b*). Use of two-stage CO_2+air treatment mode results in increased content of impurities in the carbonized specimen (Fig. 3,№ 3, Fig. 4, *c*). After MW carbonization practically all elements of mineral nutrition are found in impurities of carbon residue (Fig. 3,№ 3–5, Fig. 4, *c*–*e*). However, for specimen № 5 the impurity is localized in the form of spherical nanoparticles with diameter from 20 to 600 nm decorating the fibres (Fig. 4, *e*).

Results of quantitative analysis of elemental composition in fiber of specimen № 5 demonstrated that it mostly consists ($\sim$ 93%) of carbon. Oxygen content is low ($\sim$ 5%). The content of other elements of the impurity localized in the particles on the surface of fibers is assessed in average as less than 1% (see Table).

In our previous studies of phase composition [14] it was found that in process of carbonization in specimen (№ 3) graphite-like microcrystallites are localized: graphite with hexagonal and tetragonal crystalline lattices. Besides, the main phase in the carbonized specimen is amorphous carbon. Besides, [15] for specimen (№ 4) the formation of multi-wall carbon nanotubes (MWCNT) was found, nanoscale tubular morphology of which provides for developed specific surface of ACM, which results in adsorption capacity increase. Upon carbonization of specimen (№ 5) of cotton linter treated by MW radiation in a waveguide unit, the presence of C-graphite phase (PDF 01-089-8491) [31] was detected (Fig. 5), however, contrary to previous specimens, this phase is transient between graphite and diamond, i. e. high-temperature or formed at high pressure. Besides, graphite is not fully crystalline, and at low diffraction angles its peak is observed, and a small halo indicating partial amorphization of the specimen.

Formation of fullerene C_{70} (PDF 00-048-1206) [32] is logical due to formation of a phase transient between graphite and diamond, since high pressures are also necessary for formation of fullerenes. Apparently this happens in process of MW carbonization of the specimen, probably, as a result of rapid pressure increase in the channel due to formation of water vapors and volatile compounds. It is known that C_{70} structures have high sorption capacity [33,34], and they are much more efficient than activated carbon being an independent sorbent [35]. Fullerenes C_{70} may aggregate into agglomerates on the surface of nanofibers [36], and a similar surface pattern was observed when specimen № 5 was studied by SEM method (Fig. 6). Spherical particles on the surface of fibers have phosphates and calcium in their composition (Fig. 4, *e*), which makes it possible to presume formation of such agglomerates of fullerenes with mineral impurities.

Besides, X-ray data (Fig. 5) shows that content of calcium hydrogen phosphate phase in specimen № 5 is extremely low, which is especially noticeable compared to the previous specimens [15], however, stable hydrogen

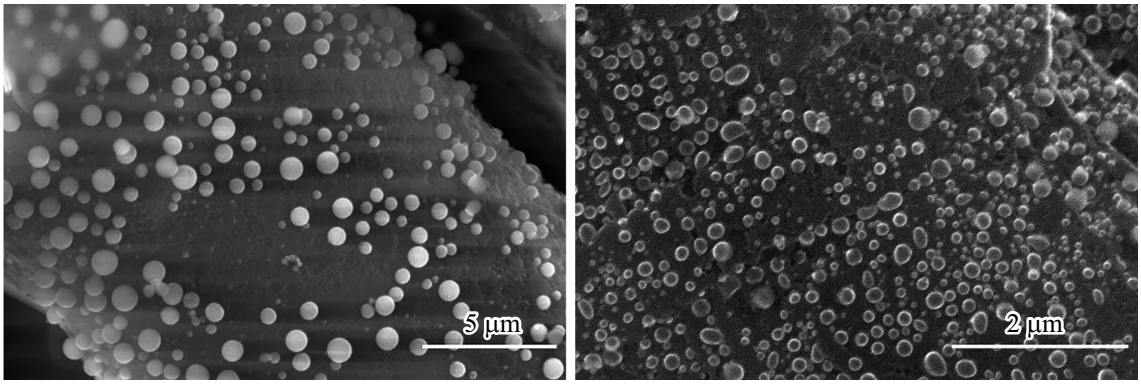

Figure 6. SEM images of fiber surface in specimen № 5.

peaks are observed along the entire length of the diffraction angles, which indicates formation of hydrogen crystallites in this specimen. Their quantity is low, and orientation in the specimen differs. This is not observed in previous specimens carbonized in a unit made on the basis of a resonating chamber. The common feature with the previous specimens is only presence of Ca (calcium) in the same phase.

Conclusion

The paper completed studies and benchmarking of features of the microwave carbonization of cotton linter specimens in a microwave chamber unit in the standing wave mode and in a microwave waveguide unit in a travelling wave mode. Based on the research of dependences of adsorption capacity and finished product mass yield it was demonstrated that MW carbonization both in chamber and waveguide units makes it possible to activate the specimens, and in one stage only, contrary to the classic thermal method. However, carbonization of cellulose specimens in a waveguide unit made it possible to obtain carbon structures containing less elements of impurities, besides, localized in particles on the surface of fibers, and not distributed in the volume. The completed studies demonstrated that the main sources of elements of impurities that may be present in the carbon residue, are the elements of mineral nutrition of plants and chemical reagents, used when preparing the specimens for the carbonization process. The most stubborn impurities identified in a carbon residue are P and Ca. Use of purer raw materials will make it possible to obtain finished activated material without additional stage of treatment, which will improve the method energy efficiency.

The results of the studies demonstrated that all specimens in the activated areas have highly porous structure of the fiber surface, besides, carbonization of cotton linter specimens treated with MW radiation caused formation of various carbon structures. During carbonization in a unit based on a resonating chamber the formation of MWCNTs was found, and in a waveguide unit the formation of fullerenes C_{70} was identified. This, in its turn, causes increased adsorption capacity of the produced activated materials.

Therefore, the data obtained in the paper from benchmarking of the properties of the carbon material from high-molecular organic raw materials carbonized by various methods confirm the prospectivity of using microwaves for the purposes of pyrolytic carbonization.

Funding

The paper was completed within the state assignment of the National Research Center „Kurchatov Institute“ (in part of optical, X-ray and electronic research) and within the assignment of the Ministry of Education and Science of Russia FNER-2022-0002 (in part of production of carbon specimens and study of the adsorption capacity).

Conflict of interest

The authors declare that they have no conflict of interest.

References

[1] J. Lin, S. Zhao, S. Cheng. Environ Sci. Pollut. Res., **29**, 48839 (2022). DOI: 10.1007/s11356-022-19334-4
[2] Y.F. Huang, P.T. Chiueh, S.L. Lo. Sustain. Environ. Res., **26**, 103 (2016). DOI: 10.1016/j.serj.2016.04.012
[3] N. Sasi Kumar, D. Grekov, P. Pre, B.J. Alappat. Renewable and Sustainable Energy Reviews, **124**, 109743 (2020). DOI: 10.1016/j.rser.2020.109743
[4] Y. Zhang, S. Fan, T. Liu, W. Fu, B. Li. Sustainable Energy Technol. Assessments, **50**, 101873 (2022). DOI: 10.1016/j.seta.2021.101873
[5] F. Motasemi, M.T. Afzal. Renewable and Sustainable Energy Reviews, **28**, 317 (2013). DOI: 10.1016/j.rser.2013.08.008
[6] S. Sathish, R. Nirmala, H.Y. Kim, R. Navamathavan. Carbon Lett., **32**, 1151 (2022). DOI: 10.1007/s42823-022-00348-4
[7] K. Chen, Z.J. He, Z.H. Liu, A.J. Ragauskas, B.Z. Li, Y.J. Yuan. Chem. Sus. Chem., **15** (21), e202201284 (2022). DOI: 10.1002/cssc.202201284
[8] D.S. Priya, L.J. Kennedy, G.T. Anand. Mater. Today Sustainability, 100320 (2023). DOI: 10.1016/j.mtsust.2023.100320
[9] Electronic source. Available at: https://www.grandviewresearch.com/industry-analysis/activated-carbon-market
[10] J.A. Menendez, A. Arenillas, B. Fidalgo, Y. Fernandez, L. Zubizarreta, E.G. Calvo, J.M. Bermúdez. Fuel Process. Technol., **91**, 1 (2010). DOI: 10.1016/j.fuproc.2009.08.021
[11] M.A.A. Zaini, M.J. Kamaruddin. J. Anal. Appl. Pyrolysis, **101**, 238 (2013). DOI: 10.1016/j.jaap.2013.02.003
[12] T. Kim, J. Lee, K.H. Lee. Carbon Lett., **15**, 15 (2014). DOI: 10.5714/CL.2014.15.1.015
[13] S.M. Villota, H. Lei, E. Villota, M. Qian, J. Lavarias, V. Taylan, I. Agulto, W. Mateo, M. Valentin, M. Denson. ACS Omega, **4**, 7088 (2019). DOI: 10.1021/acsomega.8b03514
[14] V.E. Asadchikov, I.G. Dyachkova, D.A. Zolotov, A.S. Kumskov, A.L. Vasilyev, V.V. Berestov. Crystallogr. Rep., **67** (4), 556 (2022). DOI: 10.1134/s1063774522040046
[15] I.G. Dyachkova, D.A. Zolotov, A.S. Kumskov, I.S. Volchkov, V.V. Berestov, E.V. Matveev. Phys. Usp., **66** (12), 000 (2023). DOI: 10.3367/UFNe.2023.02.039323
[16] E.M. Villota, H. Lei, M. Qian, Z. Yang, S.M.A. Villota, Y. Zhang, G. Yadavalli. ACS Sustainable Chem. Eng., **6**, 1318 (2017). DOI: 10.1021/acssuschemeng.7b03669
[17] K.Y. Foo, B.H. Hameed. Chem. Eng. J., **180**, 66 (2012). DOI: 10.1016/j.cej.2011.11.002
[18] P. Pre, G. Huchet, D. Jeulin, J.N. Rouzaud, M. Sennour, A. Thorel. Carbon, **52**, 239 (2013). DOI: 10.1016/j.carbon.2012.09.026
[19] M. Thommes, K. Kaneko, A.V. Neimark, J.P. Olivier, F. Rodriguez-Reinoso, J. Rouquerol, K.S.W. Sing. Pure Appl. Chem., **87**, 1051 (2015). DOI: 10.1515/pac-2014-1117
[20] M. Oschatz, P. Pre, S. Dörfler, W. Nickel, P. Beaunier, J.N. Rouzaud, C. Fischer, E. Brunner, S. Kaskel. Carbon, **105**, 314 (2016). DOI: 10.1016/j.carbon.2016.04.041

[21] T.C. Petersen, I.K. Snook, I. Yarovsky, D.G. McCulloch, B. O'Malley. J. Phys. Chem., **111**, 802 (2007). DOI: 10.1021/jp063973f
[22] C. Prehal, C. Koczwara, N. Jäckel, H. Amenitsch, V. Presser, O. Paris. Phys. Chem. Chem. Phys., **19**, 15549 (2017). DOI: 10.1039/C7CP00736A
[23] S. Yorgun, D. Yıldız, Y.E. Şimşek. Energy Sources, **38**, 2035 (2016). DOI: 10.1080/15567036.2015.1030477
[24] A.M. de Yuso, B. Rubio, M.T. Izquierdo. Fuel Process Technol., **119**, 74 (2014). DOI: 10.1016/j.fuproc.2013.10.024
[25] I. Demiral, C.A. Samdan. Anadolu. Univ. J. Sci. Technol. A Appl. Sci. Eng., **17** (1), 125 (2016). DOI: 10.18038/btda.64281
[26] V. Mamontov, V.N. Nefedov, S.A. Khritkin. Measurement Techniques, **61**, 723 (2018). DOI: 10.1007/s11018-018-1491-5
[27] GOST 4453-74 *Ugol aktivirovanny osvetlyayuschiy drevesny poroshkoobrazny* (Izd-vo standartov, M., 1993)
[28] A.V. Buzmakov, V.E. Asadchikov, D.A. Zolotov, B.S. Roshchin, Yu.M. Dymshits, V.A. Shishkov, M.V. Chukalina, A.S. Ingacheva, D.E. Ichalova, Yu.S. Krivonosov, I.G. Dyachkova, M. Balzer, M. Castele, S. Chilingaryan, A. Kopmann. Crystallogr. Rep., **63**, 1057 (2018). DOI: 10.1134/S106377451806007X
[29] D.A. Zolotov, V.E. Asadchikov, A.V. Buzmakov, I.G. Dyachkova, E.V. Suvorov. JETP Lett., **113**, 149 (2021). DOI: 10.1134/S0021364021030115
[30] S. Gates-Rector, T. Blanton. Powder Diffr., **34**, 352 (2019). DOI: 10.1017/S0885715619000812
[31] J. Fayos. J. Solid State Chem., **148**, 278 (1999). DOI: 10.1006/jssc.1999.8448
[32] G.V. Narasimha Rao, V.S. Sastry, M. Premila, A. Bharathi, C.S. Sundar, Y. Hariharan, V. Seshagiri, T.S. Radhakrishnan. Powder Diffr., **11**, 5 (1996). DOI: 10.1017/S0885715600008782
[33] V.V. Samonin, V.Yu. Nikonova, A.N. Kim, N.A. Grun. Izvestiya SPbGTI(TU), **8** (2010) (in Russian).
[34] E.M. Slutsker. *Adsorbtsionnye svoystva nanostrukturirovannykh uglerodnykh materialov fulleroidnogo tipa* (avtoref. kand. diss., SPbGTI(TU), SPb., 2005)
[35] V.I. Berezkin, I.V. Viktorovskii, A.Ya. Vul', L.V. Golubev, V.N. Petrova, L.O. Khoroshko. Semiconductors, **37** (7), 775 (2003). DOI: 10.1134/1.1592849
[36] T. Konno, T. Wakahara, K. Miyazawa, K. Marumoto. New Carbon Mater., **33**, 310 (2018). DOI: 10.1016/S1872-5805(18)60341-5

Translated by M.Verenikina